JOURNAL OF VIROLOGY, June 2006, p. 5577–5587 Vol. 80, No. 11
0022-538X/06/$08.00+0 doi:10.1128/JVI.00163-06

Varicella-Zoster Virus Infection of Human Foreskin Fibroblast Cells Results in Atypical Cyclin Expression and Cyclin-Dependent Kinase Activity

Stacey A. Leisenfelder and Jennifer F. Moffat*

Department of Microbiology and Immunology, State University of New York, Upstate Medical University, 750 E. Adams Street, Syracuse, New York 13210

Received 24 January 2006/Accepted 14 March 2006

In its course of human infection, varicella-zoster virus (VZV) infects rarely dividing cells such as dermal fibroblasts, differentiated keratinocytes, mature T cells, and neurons, none of which are actively synthesizing DNA; however, VZV is able to productively infect them and use their machinery to replicate the viral genome. We hypothesized that VZV alters the intracellular environment to favor viral replication by dysregulating cell cycle proteins and kinases. Cyclin-dependent kinases (CDKs) and cyclins displayed a highly unusual profile in VZV-infected confluent fibroblasts: total amounts of CDK1, CDK2, cyclin B1, cyclin D3, and cyclin A protein increased, and kinase activities of CDK2, CDK4, and cyclin B1 were strongly and simultaneously induced. Cyclins B1 and D3 increased as early as 24 h after infection, concurrent with VZV protein synthesis. Confocal microscopy indicated that cyclin D3 overexpression was limited to areas of IE62 production, whereas cyclin B1 expression was irregular across the VZV plaque. Downstream substrates of CDKs, including pRb, p107, and GM130, did not show phosphorylation by immunoblotting, and p21 and p27 protein levels were increased following infection. Finally, although the complement of cyclin expression and high CDK activity indicated a progression through the S and G_2 phases of the cell cycle, DNA staining and flow cytometry indicated a possible G_1/S blockade in infected cells. These data support earlier studies showing that pharmacological CDK inhibitors can inhibit VZV replication in cultured cells.

Varicella-zoster virus (VZV) is a member of the alphaherpesvirus family, causing chicken pox (varicella) upon primary infection and shingles (zoster) after reactivation from latency in ganglia. VZV shows a tropism for rarely dividing cell types, including differentiated keratinocytes, dermal fibroblasts, epithelium, neurons, and memory T cells (5). These cell types are typically quiescent in their in vivo states, yet VZV productively infects them all. How this large DNA virus is able to replicate its genome in an environment inhospitable to duplication is poorly understood. Less is known about the interaction of VZV with host cells compared to other alphaherpesviruses, because it is tightly cell-associated in culture and synchronous, high-multiplicity infections are not feasible.

The involvement of cellular kinases in VZV replication has recently become a topic of interest. Casein kinases I and II (CK-I and CK-II) have been found to phosphorylate the VZV glycoprotein gE, which is hypothesized to aid in cell-to-cell spread of progeny (23, 30). Glycoprotein gI was also shown to be phosphorylated by cyclin-dependent kinase 1 (CDK1) in vitro, and this phosphorylation was blocked by roscovitine, a specific CDK inhibitor (57). Our group has previously shown that roscovitine prevented VZV replication in cultured cells; however, the inhibition of glycoprotein phosphorylation was not the only mechanism of action, since early and late gene expression were also blocked (51).

CDKs are also involved in the replication of other herpesviruses. Herpes simplex virus type 2 (HSV-2), the causative agent of genital herpes, increases CDK2 activation, thus generating an environment conducive to DNA replication (26). Schang et al., using pharmacological CDK inhibitors, showed that CDKs are required for herpes simplex virus type 1 (HSV-1) DNA replication and viral gene transcription (48–50). Human cytomegalovirus (HCMV) has been shown to interact with cell cycle machinery by downregulating the pocket proteins pRb, p107, and p130, which leads to an S-phase-like environment in infected fibroblasts but blocks cellular DNA replication (11, 16, 46, 53, 54). Paradoxically, cyclin B1/CDK1 activity, normally found in late-S and G_2 phases, is increased following HCMV infection and is sustained throughout viral replication, while infected cells maintain a 2N DNA content, indicating a G_1/early-S state (47). Conscripting the activity of cellular CDKs and perturbing their cyclic regulation appear to be common strategies among herpesviruses.

Mammalian cell division is tightly regulated to avoid unscheduled or incomplete DNA replication. This regulation is primarily mediated by protein complexes each consisting of a regulatory cyclin and an enzymatic CDK. The three stages of the cell cycle are G_1, S, and G_2/M. G_1 is the preparatory stage when the cell readies itself for genomic replication and is typified by CDK4/cyclin D and CDK6/cyclin D activity (21). These complexes phosphorylate the Rb family of pocket proteins (pRb, p107, and p130), resulting in release of the E2F transcription factor family members and subsequent cyclin E transcription (17, 22, 28). CDK2 binds cyclin E, and this complex further phosphorylates pRb, resulting in a positive feedback loop of cyclin E transcription followed by ubiquitination and proteosomal degradation of cyclin E protein (1, 25, 31).

* Corresponding author. Mailing address: SUNY Upstate Medical University, Department of Microbiology and Immunology, 750 East Adams Street, Syracuse, NY 13210. Phone: (315) 464-5454. Fax: (315) 464-4417. E-mail: moffatj@upstate.edu.

The cyclin A promoter is also under the control of E2F, so when CDK2/cyclin E activity fades, CDK2/cyclin A activity takes over (52). This complex phosphorylates DNA replication machinery such as DNA polymerase α and thymidine kinase (29). CDK2 is then replaced by CDK1 (cdc2), which also binds cyclin A. CDK1/cyclin A is responsible for phosphorylating cdc6, causing its translocation out of the nucleus and thereby blocking new replication fork formation and genomic reduplication (32, 55, 56). Following DNA synthesis, cyclin B1 transcription is upregulated, protein levels increase, and cyclin B1 forms a complex with CDK1 that phosphorylates nuclear lamin components, loosening the nuclear envelope (15, 41, 44). This is a hallmark of the morphological changes occurring during the G_2 and M phases of the cell cycle. CDK1/cyclin B1 also phosphorylates Golgi proteins, including GM130, which is postulated to cause equal distribution of the organelle between daughter cells because of Golgi fragmentation (18, 34). Cyclin B1 must be degraded by the anaphase-promoting complex (APC) before the cell can undergo mitosis and complete cytokinesis (31, 44). Thus, particular CDK/cyclin complexes are active during each cell cycle phase.

We have previously shown that CDK inhibitors such as roscovitine and purvalanol inhibit VZV replication in cultured cells without directly inhibiting virally encoded kinases (35, 51). This led to our hypothesis that CDKs inhibited by roscovitine are important for VZV replication and that their activity would be altered following VZV infection of nondividing cells. We sought to investigate the effects of VZV infection on a cell's complement of cell cycle proteins, proposing that the virus would upregulate cyclin protein expression and/or CDK activity when infecting quiescent cells. We found that following VZV infection of a nondividing cell culture model, CDK and cyclin expression were upregulated and kinase complexes were activated. These changes occurred concurrently with viral protein expression, implicating them in the viral life cycle. However, the expression and phosphorylation status of various cell proteins that inhibit or activate CDKs, as well as the substrates of CDKs themselves, could not explain the high level of CDK activity and cyclin expression in infected cells. The infected cells did not appear to replicate their cellular DNA, indicating that VZV blocked normal cell cycle progression while altering the intracellular biochemical composition to aid viral DNA replication and protein synthesis.

MATERIALS AND METHODS

Propagation of cells and virus. Human foreskin fibroblasts (HFFs) (CCD-1137Sk; American Type Culture Collection, Manassas, VA), used prior to passage 18, and MeWo cells (human melanoma cell line) were grown in Eagle minimum essential medium with Earle's salts and L-glutamine, supplemented with 10% fetal bovine serum (FBS; Gemini, Woodland, CA) and nonessential amino acids. All media and supplements were purchased from Mediatech (Washington, D.C.). The recombinant parental Oka strain (rPOka) (40) was stored at −80°C and grown on HFFs for up to 10 passages. Cell-associated VZV inoculum was used in all experiments.

Viral growth curve. HFFs were grown to confluence, as determined visually using an inverted microscope (200×), and then cultured an additional 2 days to ensure quiescence. They were inoculated with VZV-infected HFFs showing more than 80% cytopathic effects (CPE) at a 1:10 ratio of infected to uninfected cells and allowed to settle for 2 hours. Cell monolayers were washed with phosphate-buffered saline (PBS) and overlaid with fresh medium. The first harvest was at this time point to calculate the initial number of infected cells. The monolayers were harvested with trypsin-EDTA each day postinfection for 7 days and resuspended in 10 ml of medium, and the titers were determined by standard infectious-focus assay as referenced, with the exception that melanoma cells were used instead of Vero cells (36).

Flow cytometry. Confluent HFFs were released from contact inhibition by a 1:3 split into new flasks. Uninfected cultures were harvested every 2 hours postplating and fixed in ethanol for a total of 32 h as in reference 51, and mock- or VZV-infected cultures were harvested 5 days postinfection (p.i.). Briefly, cell monolayers were trypsinized, fixed with 70% cold ethanol, and incubated with RNase A (Sigma, St. Louis, MO); DNA was stained with propidium iodide (PI; Sigma); and fluorescence from PI-DNA complexes was determined using an LSR II flow cytometer and analyzed using FACSDiva software (Becton Dickinson Information Systems, San Jose, CA). 2N DNA content was taken as cells in G_0/G_1, 4N as a G_2 cell population, and cells in between as being in S phase; all cells to the left of the G_1 peak were analyzed as sub-G_1. Percentages of cells expressing VZV proteins were compiled using the same fixation method, followed by permeabilization with Triton X-100 and staining with antisera to VZV (generously provided by Ann Arvin, Stanford University) and fluorescein isothiocyanate-conjugated antihuman antibody prior to PI staining. Negative controls included unstained cells and cells stained with only secondary antibodies.

Immunoblotting. Monolayers were scraped into ice-cold RIPA buffer (50 mM Tris-HCl, pH 7.4; 1% NP-40; 150 mM NaCl; 1 mM EDTA; 1 mM Na_3VO_4; 1 mM NaF; supplemented with protease inhibitor tablets [Roche, Indianapolis, IN]), lysed by rocking at 4°C, and clarified by centrifugation at 14,000 × *g* for 15 minutes. The supernatants were frozen at −20°C. Proteins were also extracted from intact cells using sample buffer (166 mM Tris-HCl, pH 6.8; 7% sodium dodecyl sulfate [SDS]; 0.3% bromophenol blue; 33% glycerol; 0.3 M dithiothreitol) in parallel cultures to ensure complete disruption of cellular components as in reference 6; the extraction methods gave reproducible and similar results (data not shown). Protein concentrations of RIPA extracts were measured using the Bradford assay (Bio-Rad Laboratories, Hercules, CA) (7). Equal amounts of proteins were electrophoretically separated on 12% SDS-polyacrylamide gel electrophoresis (SDS-PAGE) gels (6% gels for pRb, p107, and p130), transferred to polyvinylidene difluoride membranes, and probed with antibodies to the following proteins: CDK1 (sc-54), CDK2 (sc-163), CDK4 (sc-260), CDK6 (sc-177), cyclin A (sc-751), cyclin B1 (sc-752), cyclin B2 (sc-22776), cyclin D1 (sc-246), cyclin E (sc-481), p107 (sc-318), p130 (sc-9963 and sc-317), cdc25A (sc-7157), cdc25B (sc-5619), cdc25C (sc-327), p21 (sc-397), p27 (sc-1641), and GM130 (sc-16268) (Santa Cruz Biotechnologies, Santa Cruz, CA), cyclin D2, cyclin D3, p130, β-actin (Sigma), pRb (Pharmingen, San Diego, CA), and VZV human serum (generously provided by Ann Arvin, Stanford University). Secondary antibodies conjugated to alkaline phosphatase or horseradish peroxidase were purchased from Jackson ImmunoResearch Laboratories, Inc. (West Grove, PA). Alkaline phosphatase secondary antibodies were developed using Lumi-Phos detection reagent and horseradish peroxidase secondaries using SuperSignal West Dura substrate (Pierce Biotechnology, Rockford, IL) and visualized using Kodak BioMax MR film (Amersham Biosciences, Piscataway, NJ). Quantitative results were obtained by densitometry of the developed film, comparing each band to β-actin.

Immunoprecipitation/kinase assays. Using the samples harvested in RIPA buffer, proteins were immunoprecipitated as follows. All lysates were precleared using rabbit immunoglobulin G (IgG) and the appropriate bead conjugate. Lysates were incubated with antibody first (CDK2- or CDK1-protein A+ agarose beads; Pierce Biotechnology, Rockford, IL), or antibody was conjugated to the beads (CDK4-ExactaCruz F matrix; Santa Cruz Biotechnology) (cyclin B1-protein A+ agarose beads; Pierce Biotechnology) overnight at 4°C. Lysate/antibody complexes or bead/antibody complexes were then combined with beads and lysate, respectively, for 3 hours at room temperature, followed by extensive washing with cold RIPA buffer. Each sample was divided in half, with one aliquot then equilibrated to kinase assay buffer (50 mM Tris [pH 7.5], 10 mM $MgCl_2$, 2.5 mM EGTA, 1 mM dithiothreitol, 0.1 mM ATP, 1 μCi [γ-^{32}P]ATP) and the appropriate substrate (0.5 μg pRb fragment [Santa Cruz Biotechnology] for CDK4 and 50 ng histone H1 [Upstate Biotechnology, Lake Placid, NY] for CDK2 and cyclin B1) for 30 minutes at 37°C. The reaction was stopped by the addition of sample buffer, and proteins were boiled off the beads, separated on 10% SDS-PAGE gels, dried, exposed to a phosphorimaging cassette, and analyzed using a PhosphorImager and ImageQuant software (Molecular Dynamics, Sunnyvale, CA). The other aliquot was tested for IP efficiency by boiling all proteins off the beads with sample buffer, followed by immunoblotting on 12% SDS-PAGE gels as described above.

Immunofluorescence microscopy. Confluent monolayers of HFFs grown on four-well chamber slides were mock infected with HFFs or infected at a 1:30 dilution with VZV grown in HFFs for 48 h. Slides were fixed in cold acetone: methanol (vol/vol, 1:1) for 20 minutes at −20°C and allowed to air dry. Following

rehydration in PBS, autofluorescence was quenched using 0.1% sodium borohydride (Sigma) in PBS for 15 minutes at room temperature with agitation every 5 minutes. Cells were blocked with 10% donkey serum and incubated with antibodies to cyclin B1 (sc-7393; Santa Cruz Biotechnology), cyclin D3 (C7214; Sigma), and IE62 (generously provided by Paul Kinchington, University of Pittsburgh) followed by a mouse-specific secondary antibody conjugated to Texas Red isothiocyanate (Texas Red isothiocyanate α-mouse) or a rabbit-specific antibody conjugated to fluorescein isothiocyanate (fluorescein isothiocyanate α-rabbit; Jackson ImmunoResearch, West Grove, PA). DNA was stained with TO-PRO-3 (Molecular Probes, Eugene, OR). Control staining was done using isotype-matched serum in place of primary antibodies, followed by the appropriately conjugated secondary. Images were taken on a Bio-Rad MRC 1024 confocal laser scanning microscope and analyzed using the LaserSharp program. Images were taken at the same laser intensities and confocal specifications between mock-infected, infected, and control-stained wells.

RESULTS

VZV growth in nondividing HFFs. VZV replication is restricted to human and monkey cells, and many cell lines used to propagate the virus are derived from carcinomas in which the cell cycle is perturbed. Thus, primary HFFs were selected for these studies since they become contact inhibited when grown to confluence, which mimics their quiescent state in the dermis, and their cell cycle machinery is regulated normally. The standard model for VZV replication uses rapidly dividing melanoma cells (MeWo cells), so we had to ensure that VZV could grow to similar titers in confluent HFFs. Replicate cultures of subconfluent MeWo cells or confluent HFFs were infected with a 1:10 (infected:uninfected cells) dilution of VZV rPOka, a low-passage, recombinant isolate of the parental vaccine strain (40), grown in HFFs. After adsorption for 2 h, a sample was taken to represent the inoculum at day 0, and subsequent samples were collected daily for 1 week. The extent of VZV cell-cell spread was determined by infectious focus assay on MeWo cells because these cells grow quickly and produce large, round plaques. Confluent HFFs were susceptible and permissive for VZV replication, as indicated by logarithmic growth of virus during the first 2 days p.i. (Fig. 1A). In fact, peak titers were significantly higher ($P < 0.05$) in HFFs after 5 and 6 days p.i. than those of virus grown in subconfluent melanoma cells. A focus of VZV-infected cells surrounded by uninfected cells shows the CPE in HFFs: rounded cells, increased refractory index, and an apparent absence of syncytia that is commonly observed with VZV-infected MeWo cells (Fig. 1B). Contact-inhibited HFFs supported VZV replication to titers equivalent to those of rapidly dividing cells and were used for the remainder of this study.

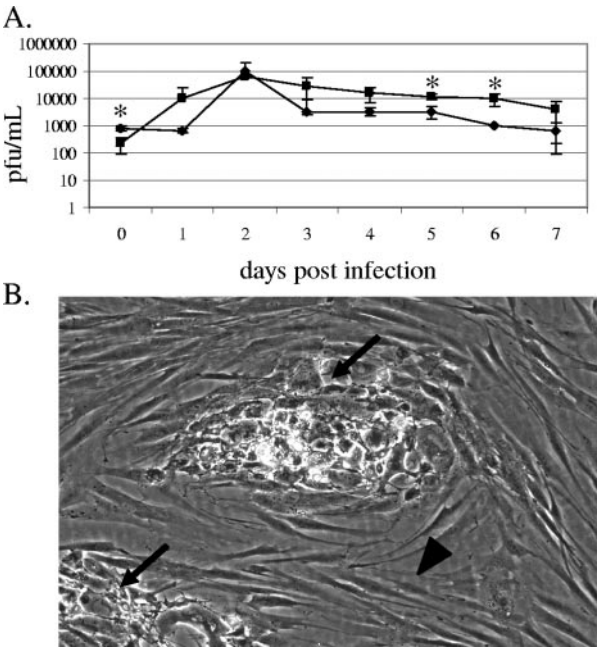

FIG. 1. Kinetics and cytopathic effects of VZV replication in confluent human fibroblasts. (A) HFFs (filled squares) were grown to confluence, or MeWo cells (filled diamonds) were grown to 60% confluence, and inoculated with a 1:10 dilution of VZV rPOka-infected HFFs. Virus input was measured at 2 h p.i. (indicated by day 0), and cell-to-cell spread was measured daily by standard plaque assay. The titer of each sample was determined in triplicate and the experiment was repeated twice; error bars indicate the standard deviations, and the asterisks represent significant differences as measured by Student's *t* test ($P < 0.05$). (B) Phase-contrast micrograph of a VZV plaque in HFFs 2 days p.i. (magnification, ×200). The normal spindle appearance of uninfected HFFs (arrowhead) is in contrast to the increased refractory index and spherical morphology of infected cells (arrows).

VZV infection of quiescent HFFs induces cyclin B1 and D3 protein expression. Very little is known about normal CDK and cyclin expression in HFFs, because they are primary cells that have not been studied as intensively as tumor cells. In addition, typical cell synchronization methods, including those involving nocodozole and mimosine, could not be used because the drugs were cytotoxic for HFFs even at very low concentrations (authors' observations). Instead, the timing of the cell cycle and expression patterns of CDKs and cyclins were determined by culturing HFFs to confluence and then diluting the cells into new flasks and fresh medium to induce partially synchronized division. Samples were collected at various times postplating for analysis of DNA content by propidium iodide staining and flow cytometry and for measurement of protein expression by immunoblotting. Four hours after growth induction, 78.7% of the cells were in G_1 phase; 24 h postplating, 11.3% were in S; and 23.7% were in G_2/M after 28 h (Fig. 2C and Table 1). The cells in these populations were approximately 70% confluent by phase-contrast microscopy at each time point (data not shown). The CDK and cyclin immunoblot profiles of uninfected, cycling HFFs corresponded to the cell cycle profiles obtained by DNA content analysis. Immunoblotting confirmed that HFFs were cycling semisynchronously, as CDK1 and cyclins A and B1 were present 24 and 28 h postplating, which indicates that some cells were in late-S or G_2 phases (Fig. 2A and B, lanes 1 to 3). The CDK2 antibody distinguished between active and inactive kinase, as it has been shown that a faster-migrating form of this protein is active and the slower-migrating form is inactive (24), and a faster-migrating band appeared at 24 h (Fig. 2A, lane 2). Cyclin D3 was present throughout all phases, since expression of this protein is serum dependent and the cells were cultured in media containing 10% FBS. The amounts of total CDK4 and -6 did not change. Cyclin E expression was detected at 4 and 28 h.

When HFF monolayers reach confluence, the cells stop dividing and, as such, should not express cyclins A or B1 or active CDKs. It was not known whether VZV affected the level or activity of these regulatory proteins or caused the cells to enter

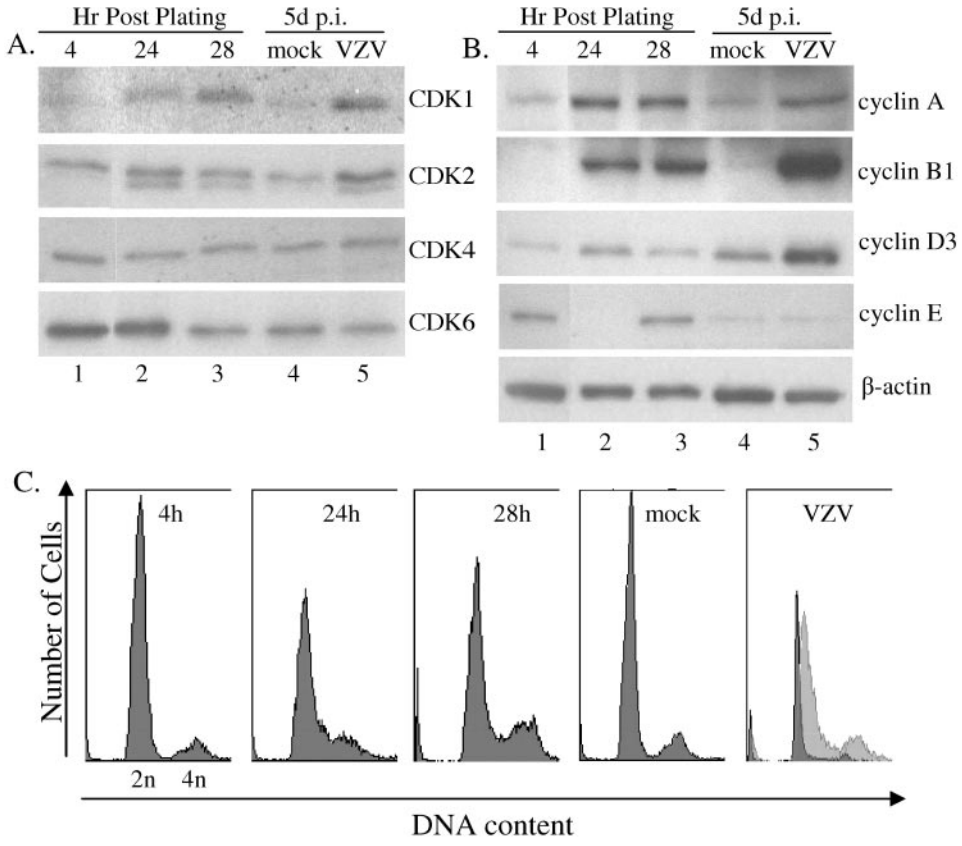

FIG. 2. Analysis of CDKs, cyclins, and DNA content in normal and VZV-infected HFFs. Immunoblots of CDKs (A) and cyclins (B) in uninfected, cycling control cells and mock-infected and VZV-infected HFFs. Control HFFs were grown to confluence, split 1:3 to stimulate cell division, and then harvested 4 h (lane 1), 24 h (lane 2), and 28 h (lane 3) postplating. Confluent HFF monolayers were mock inoculated with HFFs (lane 4) or inoculated with VZV-infected HFFs (lane 5) at 1:10 ratios and cultured until CPE were greater than 80% (5 days). β-Actin levels were used as a loading control. An intervening lane between lanes 1 and 2 was deleted from the image using Adobe Photoshop. (C) Flow cytometry analysis of cells stained with propidium iodide and antisera to VZV. Number of cells is indicated on the *y* axis, and DNA content (propidium iodide mean fluorescence intensity) is on the *x* axis. In the VZV histogram (right panel), VZV-positive cells are shown in the light gray area and VZV-negative cells from the same culture in the dark gray area. All samples were analyzed using the same parameters in two separate experiments; representative histograms are shown.

the cell cycle. Confluent HFFs were infected or mock infected until more than 80% of the infected culture showed CPE, approximately 4 to 5 days p.i., and were harvested for immunoblotting. As expected, mock-infected cultures showed the typical complement of proteins for nondividing cells: cyclin D3 was expressed, but there were negligible amounts of cyclins A, B1, and E; all CDKs were detected, but CDK2 was detected only as the slower-migrating, presumably inactive form. Upon VZV infection, CDK1, CDK2, and cyclin A, B1, and D3 levels increased concurrently, and CDK2 appeared as the faster-migrating, active form (Fig. 2A and B). When the immunoblot analysis was repeated with serum-starved cultures (1% FBS), similar increases in cyclin B1 and D3 protein were observed at 5 days p.i. (data not shown), indicating that this was not an artifact of exogenous growth stimulation. There was no difference between mock-infected and VZV-infected HFFs in regard to CDK4, CDK6, or cyclin E protein expression.

TABLE 1. Cell cycle analysis of partially synchronized HFFs and VZV-infected cultures

Condition	Proportion of cells in phase (%)				Total (%)
	Sub-G_1	G_1	S	G_2/M	
4 h postplating	10.9	78.7	1.6	8.8	100.0
24 h postplating	13.3	61.6	11.3	13.0	99.2
28 h postplating	4.9	59.4	10.7	23.7	98.7
Mock infected	2.4	78.6	2.6	14.0	97.6
VZV infected[a]	3.6	68.2	8.2	16.0	96.0

[a] Only cells which stained positive for VZV glycoproteins were contained in analysis of cell cycle phases.

The aberrant pattern of cyclin expression suggested that VZV-infected cells were progressing through the cell cycle, possibly with a G_2/M arrest as indicated by the high cyclin B1 protein expression. To determine whether VZV-infected HFFs were duplicating cellular DNA, flow cytometry of propidium iodide-stained cultures was performed. Infected cultures were also stained with an antibody to viral glycoproteins and gated from the surrounding, uninfected cells, which express no viral late proteins. Figure 2C indicates the DNA content of infected cells (light gray histogram) and uninfected cells (dark gray histogram) from the same culture. Although there is a slight increase in the G_2 population of VZV-infected

HFFs (16.0% compared to 14.0% in the mock-infected population), this alone cannot explain the elevated expression of cyclin B1. Normal, cycling HFFs contained more cells in G_2 (23.7%) at 28 h postplating, yet expressed less cyclin B1 than VZV-infected HFFs. Thus, VZV-infected HFFs did not appear to completely replicate cellular DNA, and the increase in cyclin B1 protein in infected cells can be attributed to effects of the virus and not to a G_2/M arrest.

We attempted to study the cell cycle profile in MeWo cells. However, mock-infected MeWo cells expressed high levels of all CDKs and cyclins examined, and there was no significant difference when they were infected with VZV (data not shown). Since this cell type is asynchronously and rapidly dividing and does not cease replication when confluent, it was not an adequate cell type to use to simulate the conditions which VZV encounters in vivo.

VZV-induced increases in CDK and cyclin proteins occur concurrently with VZV replication. Single-step VZV growth curves are not feasible since there is not enough cell-free VZV produced to synchronously infect a cell monolayer at a multiplicity of infection of 1. Because simple kinetics of VZV replication and its influence on cell cycle proteins cannot be done, we attempted to demonstrate a causal relationship between VZV glycoprotein synthesis and cellular protein changes over a period of 3 days. Infected HFFs were stained for VZV glycoproteins and flow cytometry was done to calculate the percentage of the culture expressing VZV proteins. The inoculum resulted in 7.2% of the culture expressing VZV proteins at time zero, as determined by flow cytometry, and increased steadily throughout the experiment to a peak of 68.8% infection by day 3 (Fig. 3, percentages beneath the VZV glycoprotein panel). Confluent HFFs were either mock- or VZV-infected as described above, and the entire culture was harvested from zero to three days p.i. for immunoblotting for each CDK and cyclin, as well as for VZV glycoproteins and β-actin (Fig. 3). Densitometry of each band was normalized to that of β-actin to calculate the approximate amount of protein and was then compared to the mock-infected control at each time point to yield increases (as *n*-fold of the control); samples were collected in three replicates for statistical analysis, and representative immunoblots for each protein are shown. Cyclin D3 and CDK1 increased as early as 1 day p.i. and peaked at 3 days p.i.; samples from days 4 through 7 p.i. did not show an increase above that of 3 days p.i. for any immunoblot (data not shown). Cyclin B1 increased steadily through 3 days p.i., resulting in a sixfold increase over that of the mock-infected group. Cyclin A also demonstrated a threefold increase over that of the mock-infected control at 3 days p.i. Cyclin E levels remained equal in all samples, with a slight increase by 3 days p.i.; this blot was overexposed to show equal protein in each lane. CDK1 showed significant increases after 1 day p.i. and 3 days p.i., while CDK2 levels remained constant. The increase of CDK1 and the cyclins on day 3 is concurrent with the maximal titers of VZV from confluent HFF cultures (Fig. 1A). Variability in the cell cycle protein content in the inoculum at day zero is responsible for the variability in average values at that time point. These changes in cell cycle protein concentration correlated with increasing VZV protein synthesis and replication, as indicated by immunoblotting and flow cytometry for VZV glycoproteins.

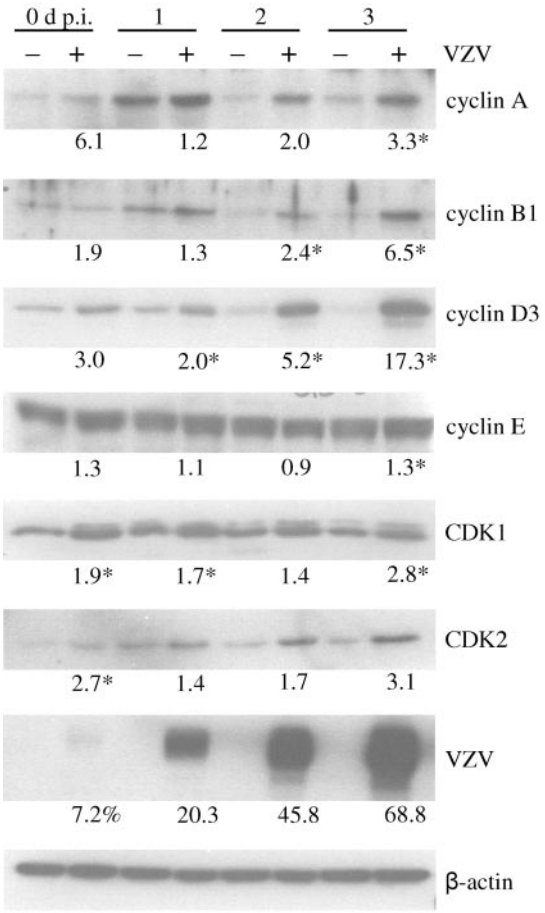

FIG. 3. Kinetics of CDK and cyclin expression in VZV-infected HFFs. Confluent HFF monolayers were mock inoculated with HFFs or inoculated with VZV-infected HFFs at 1:10 ratios. Cells were harvested 2 h (0 d), 1 day, 2 days, and 3 days p.i. and analyzed by immunoblotting for CDK and cyclin levels. VZV glycoproteins were detected using human serum from a patient with a high VZV titer (courtesy of Ann Arvin, Stanford University) and the percentages of VZV-positive cells by flow cytometry are shown. The average changes (*n*-fold) in CDK and cyclin levels compared to those in mock infection are shown below each panel and were normalized to β-actin. An asterisk indicates a significant difference between VZV- and mock-infected cells at that time point (Student's *t* test, $P < 0.05$). Three separate experiments were performed for densitometry analysis; representative blots are shown. +, VZV positive; −, VZV negative.

CDKs are active following VZV infection of nondividing HFFs. CDKs and cyclins combine to form heterodimers that phosphorylate cellular targets needed for DNA replication and cell division. The increase in cyclin protein expression and the apparent absence of total cellular DNA replication in VZV-infected HFFs raised the question of whether the CDK/cyclin complexes were active. Using samples collected on day 5 p.i., immunoprecipitation/kinase assays were performed to determine whether these kinases were active in VZV-infected cells. Proteins were immunoprecipitated from mock- or VZV-infected HFFs, incubated with the appropriate substrate (histone H1 for CDK2 and cyclin B1, pRb fragment for CDK4) and [γ-^{32}P]ATP (Fig. 4). Mock-infected samples exhibited CDK2 activity and undetectable CDK4 activity. However, upon infection with VZV, CDK4 phos-

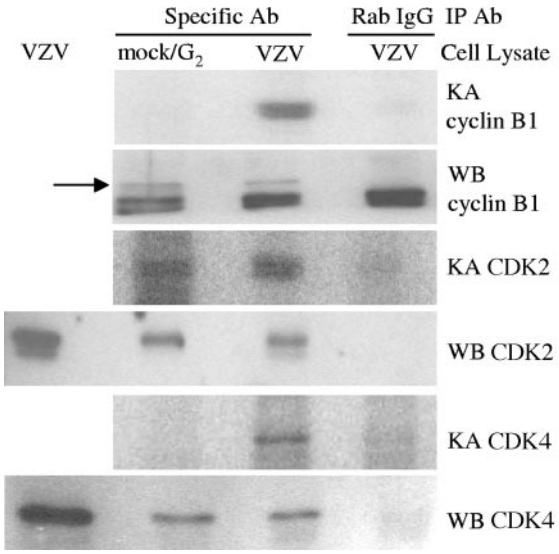

FIG. 4. Kinase assays of CDKs in mock- and VZV-infected HFFs. Confluent HFF monolayers were mock inoculated with HFFs or inoculated with VZV-infected HFFs at 1:10 ratios and then cultured until CPE were greater than 80% (5 days). Cell lysates were collected in RIPA buffer, protein concentration was determined, and equal amounts were immunoprecipitated with the indicated antibodies. Kinase reactions (KA) were performed with assay buffer containing the appropriate substrate (histone H1 for CDK2 and cyclin B1 or a pRb fragment for CDK4 and CDK6) and [γ-^{32}P]ATP. A parallel aliquot was analyzed by immunoblot (WB) for immunoprecipitation efficiency; in the cyclin B1 immunoblot panel, the arrow indicates cyclin B1 protein while the lower band is the heavy chain of the precipitating antibody. The negative control is an immunoprecipitation with rabbit IgG using VZV-infected lysates. These results are representative of three separate experiments for CDK4 activity, two separate experiments for cyclin B1 and CDK6, and four separate experiments for CDK2 activity. Ab, antibody; Rab, rabbit.

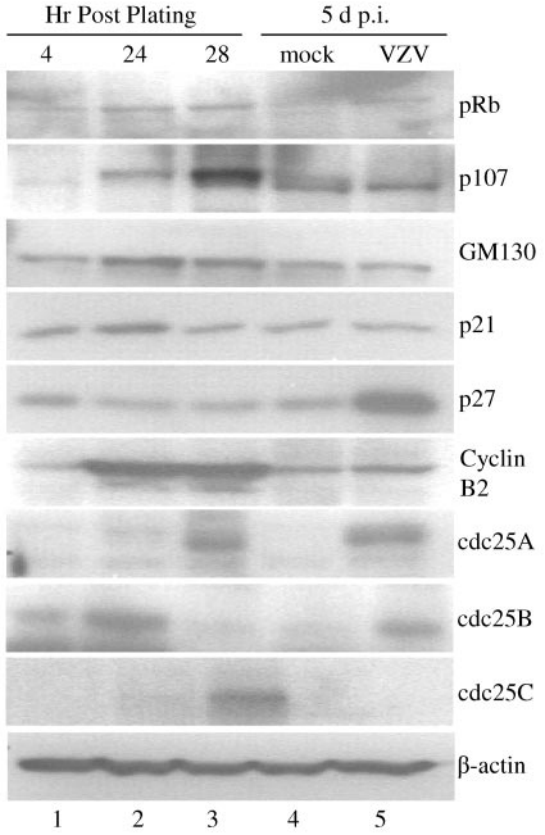

FIG. 5. Immunoblots of cellular CDK inhibitors, activators, and substrates. Cycling HFF controls (4, 24, and 28 h postplating, lanes 1 to 3) and 5-day-p.i. mock-infected (lane 4) or infected HFFs (lane 5) were harvested in sample buffer. Lysates from equal numbers of cells were added to each lane, and comparable levels of β-actin indicated equal protein loading. The immunoblots were performed at least twice using samples obtained from two separate experiments; representative blots are shown.

phorylated a pRb fragment, and CDK2 kinase activity was sustained. CDK1 activity was also measured, but the results were equivocal due to nonspecific histone H1 kinase activity (which was not CDK activity, since immunoblotting failed to detect CDK protein) that associated with the immunoprecipitation beads in the lysates of VZV-infected cells (data not shown). Instead, we opted to analyze the kinase activity associated with cyclin B1, which is normally partnered with CDK1. HFFs synchronized 28 h postplating were used as a control, as they express cyclin B1 and mock-infected cells do not, and an immunoprecipitation with rabbit IgG was used as a negative control. Kinase activity was present only when cyclin B1 was precipitated from VZV-infected cell lysates, indicating that this protein was associated with an active kinase in infected cells. The absence of cyclin B1-associated kinase activity in the 28-h HFFs is likely due to having missed the brief spike of CDK1 activity at the end of S phase; 28 h postplating is probably late-G_2/M phase, where cyclin B1-associated kinase activity is inhibited to allow final cell division (37, 41). CDK6 did not demonstrate pRb-kinase activity using multiple replicates of mock- or VZV-infected HFF lysates and ATP concentrations (data not shown). Immunoblots for CDKs were performed on each immunoprecipitation to ensure that equal amounts of protein were present. Although negligible kinase activity was observed in mock-infected cells, CDK or cyclin B1 protein was detected in each reaction. To rule out nonspecific binding of kinases to the antibodies or beads, rabbit IgG was used in control immunoprecipitations with VZV-infected lysates; there was no nonspecific CDK binding to rabbit IgG or the beads. Thus, VZV infection of quiescent HFFs resulted in sustained CDK2 activity, induced CDK4 activity, absence of CDK6 activity, and activation of histone kinase(s) associated with cyclin B1.

VZV-induced cell cycle dysregulation extends to regulators and substrates of CDKs. CDKs and cyclins are regulated by a complex network of activators and inhibitors, all of which could be affected by VZV infection. Moreover, it was not known whether the active CDKs were phosphorylating their typical substrates within infected cells, only that they were active in vitro. To address this question, immunoblots were performed to analyze the levels of CDK inhibitor proteins (CKIs), phosphatases, and substrates. The main CKIs of CDK1 and CDK2 are p21 and p27, and CDK activity can be stimulated by degradation of p21 and p27 (reviewed in reference 38). Immunoblots of p21 and p27 showed no decrease in protein expression between mock-infected and infected cultures, indicating that increased CDK activity was not due to loss of these CKIs (Fig. 5). To the contrary, p27 levels increased in VZV-infected HFFs compared to mock-infected

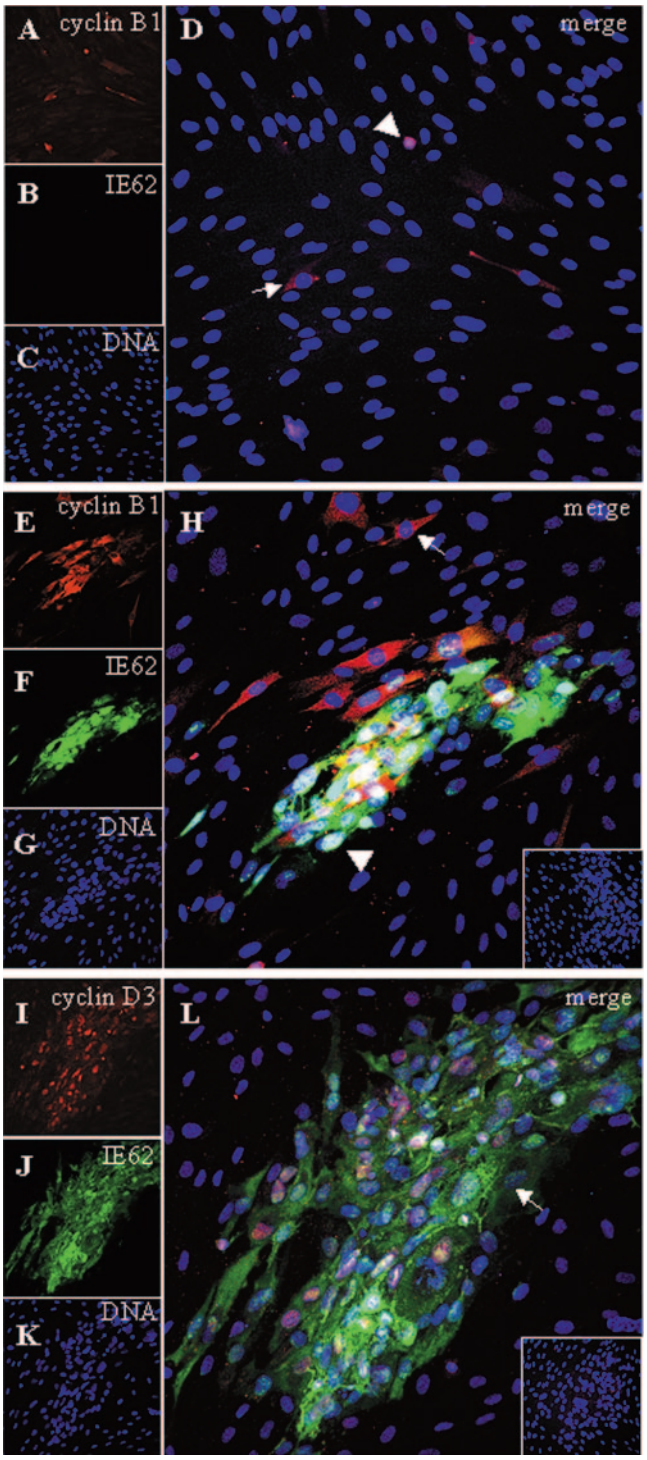

FIG. 6. Localization of cyclin B1 and cyclin D3 in VZV-infected HFFs. HFFs were grown to confluence on chamber slides and infected with a 1:30 dilution of VZV rPOka/HFFs or mock infected with HFFs for 48 h. Monolayers were fixed with cold acetone-methanol and treated with antibodies to detect cell and virus proteins. (A to D) Mock-infected confluent HFFs stained for cyclin B1 (red, panel A), IE62 (green, panel B), and DNA (blue, panel C); and a merged image (D). (E to H) VZV-infected confluent HFFs stained for cyclin B1 (red, panel E), IE62 (green, panel F) and DNA (blue, panel G); and a merged image (H). The arrows indicate cyclin B1 expression in the cytoplasm of a cell devoid of IE62 protein (uninfected); the arrowheads show IE62 expression without cyclin B1 (infected). (I to L) VZV-infected confluent HFFs stained for cyclin D3 (red, panel I), IE62 (green, panel J) and DNA (blue, panel K); and a merged image (L). The arrow in panel L indicates a cell positive for IE62 staining and negative for cyclin D3. Negative controls (insets, H and L) show infected cells treated with isotype-specific animal sera, appropriate secondary antibodies, and the DNA stain. Images were formatted using LaserSharp. Magnification, ×200. These images are representative of more than 50 plaques examined from three different experiments.

controls, so CDK activity was not a direct result of CKI degradation.

Full CDK activity requires the removal of inhibitory phosphates by the cdc25 family of phosphatases. Cycling HFFs contained cdc25C only at 28 h postplating, consistent with its published activity as a G_2/M regulator, and no cdc25C was detected in mock-infected or infected cells (Fig. 5, lanes 3 to 5). Cdc25A was detected at 28 h in the control sample, and it was more abundant in the infected cells than the mock-infected cells (Fig. 5). Cdc25B was detected in the 4- and 24-h cultures, as well as that of VZV-infected cells.

To determine whether VZV was selectively inducing the expression of cyclins involved in proliferation, we analyzed cyclin B2, a Golgi protein whose expression is independent of the cell cycle. Cyclin B2 protein increased 24 and 28 h postplating, which was expected since the Golgi apparatus increases in size and begins to fragment during this time (45). However, unlike cyclin B1, cyclin B2 was not expressed at higher levels in the VZV-infected culture than the mock-infected cells (Fig. 5). These results indicate that cyclin upregulation was not global for all family members.

Because of the increased CDK activity in infected HFF samples, we investigated the primary targets of CDKs. p107 expression was low 4 h postplating, increased by 24 h, and peaked at 28 h, with increasing phosphorylation evidenced by a slower-migrating band (Fig. 5, lanes 1 to 3). In VZV-infected samples, where CDKs were highly active by in vitro kinase assay, p107 was detected only in the under-phosphorylated form, indicating that it was not a CDK target. It is possible that p107 is phosphorylated in infected cells and then quickly degraded; however, our ability to detect mobility shifts in cycling HFFs indicates that this would not be the case. Similarly, there was no difference in the amount or migration of pRb between mock-infected and infected samples, indicating that it was not phosphorylated by CDKs present in VZV-infected cells (Fig. 5). The third pRb family member, p130, could not be detected in any samples, whether extracted with RIPA or sample buffer, using commercially available antibodies (data not shown). GM130, a Golgi protein that is a substrate of CDK1, showed no difference in expression or mobility between mock- or VZV-infected cultures (Fig. 5). Thus, the high CDK activity found in VZV-infected HFFs by kinase assay was not directed toward the expected cellular substrates and could not be directly attributed to alterations in the proximal regulators (CKIs) but could be a result of increased cdc25A and B phosphatase expression.

Cyclins D3 and B1 are present in infected plaques. In order to confirm that expression of cyclins B1 and D3 was limited to areas of viral infection and to investigate subcellular localization, indirect immunofluorescence confocal microscopy was

performed. In mock-infected confluent monolayers of HFFs, cyclin B1 was detected in a small number of cells (Fig. 6A to D). Where cyclin B1 (shown in red) was cytoplasmic (Fig. 6D, arrow), these cells were presumably arrested in G_2/M phase. Where cyclin B1 was in the nuclei of rounded cells (magenta), they were in S/G_2 phase and undergoing cell division after settling upon the monolayer (Fig. 6D, arrowhead). Thus, cyclin B1 was detected in scattered HFFs. In contrast, cyclin B1 expression was concentrated in and around VZV plaques and showed both cytoplasmic and nuclear localization (Fig. 6E to H). Cells with cytoplasmic cyclin B1 (red) were found within VZV plaques, surrounding the plaques, and also in uninfected areas (arrow). Similarly, there were cells that synthesized IE62, a VZV immediate-early protein, but no cyclin B1 was present (cells with green and blue only, arrowhead). However, toward the center of the plaque, cyclin B1, IE62, and DNA (blue) colocalized, appearing as white in the merge panel (Fig. 6H). Indeed, all three possible dual combinations of protein colocalization were observed: IE62 with cyclin B1 in the cytoplasm (yellow), IE62 with DNA (teal), and cyclin B1 with DNA (magenta).

Unlike cyclin B1, cyclin D3 was not detectable in mock-infected HFF monolayers by microscopy (data not shown). However, cyclin D3 expression noticeably increased in infected cells and was limited to the nuclei of VZV-infected cells (Fig. 6I to L). This was indicated by white areas in the merged images where cyclin D3 (red) and IE62 (green) colocalized with DNA (blue). Colocalization in the cytoplasm, indicated in yellow, was nearly absent. IE62 expression preceded cyclin D3, since the VZV protein appeared as punctate nuclear spots in cells at the edges of the plaques where no cyclin D3 was detectable (arrows). In contrast to cyclin B1, which was expressed in the absence of IE62 in some cells, cyclin D3 was not detected in cells that did not express IE62. This suggests that cyclin D3 overexpression depended on VZV infection.

DISCUSSION

The main finding of this study is that VZV infection of quiescent HFFs results in dysregulated cyclin expression and CDK activity. This supports the contention that herpesviruses selectively alter cell cycle proteins to create an environment that allows viral genome replication while cellular DNA synthesis is hindered. Resting cells typically have low CDK activity whereas herpesviruses appear to need higher levels of CDK activity, since pharmacological CDK inhibitors block viral replication (10, 50, 51). By using quiescent, contact-inhibited HFFs as a model system, we have shown that host cells do not need to be actively dividing to accommodate VZV replication, nor does VZV replicate to higher titers in dividing cell types (Fig. 1A).

The DNA content of infected cells remained at 2N, indicating a G_1/S state, while the profile of CDKs and cyclins was atypical. CDKs 2 and 4 and a cyclin B1-associated kinase are active simultaneously, as indicated by in vitro kinase assays (Fig. 4). Uninfected, cycling HFFs followed predictable patterns of cyclin production and destruction, with cyclin E present early in the cell cycle and cyclin A and B1 upregulated later (Fig. 2B). In contrast, VZV-infected HFFs demonstrated sustained increases in cyclins A, B1, and D3 that corresponded with virus spread through the cell monolayer (Fig. 3). This suggests that VZV specifically upregulates these proteins for its own replication. The induction of cell cycle proteins cannot be attributed to cells surrounding the plaque dividing to fill the gaps, since VZV-infected cells do not begin to lift off the cell culture surface until at least 7 days p.i. (authors' observations). Moreover, cells in the infected cultures were not entering G_2 phase, since neither the VZV-negative nor the VZV-positive cells showed an increase in the 4N population by flow cytometry. This evidence suggests that cells surrounding VZV plaques are not entering or completing S phase. Finally, VZV does not induce apoptosis in infected confluent HFFs, as demonstrated by the absence of a significant sub-G_1 peak that would indicate DNA fragmentation and the lack of condensed chromatin by 4′,6′-diamidino-2-phenylindole (DAPI) staining (authors' observations). In addition, the G_1 peak of infected cells is wider than that of the surrounding, uninfected cells. This could be a result of the 125-kb VZV DNA genome replicating within these cells and being labeled with PI; each infected cell contains more total DNA than do mock-infected controls, with the possibility of thousands of VZV genomes in a single cell. This could either be the result of cells with different numbers of VZV genomes or the infected cells entering early S phase and replicating cellular DNA. Flow cytometry and PI staining are unable to distinguish between cellular and viral DNA, so this question remains unanswered.

The atypical expression of cyclins A, B1, and D3 in VZV-infected HFFs was also reflected in unusual patterns of CDK and histone H1 kinase activity. The kinase activity associated with cyclin B1 was taken as a correlate of CDK1 activity because CDK1 activity could not be measured directly. What is striking is that active forms of CDK1 and CDK2 would be present simultaneously in VZV-infected cells. There is no point in the normal cell cycle where CDK1 and CDK2 are active at the same time, as this would perturb the sequential phosphorylation of substrates that govern DNA synthesis and mitosis, respectively, and could cause aneuploidy and reduplication of the genome. This did not seem to occur in infected cells, since the DNA content remained at 2N, indicating a G_0/G_1 state (Fig. 2C). Although there is some similarity in DNA profiles between HFFs in S phase (24 h postplating) and VZV-infected HFFs after 5 days p.i. (Fig. 2C), this would not explain the high cyclin B1 levels. Cyclin B1 should only be expressed after the cellular genome has been replicated, in early G_2 phase, and there is no significant increase in the percentage of cells with 4N DNA content, an indicator of G_2/M phase.

Because cell-free VZV is a misnomer (culture supernatants contain negligible intact virions, and lysing cells merely reduces infectivity), it is not feasible to synchronously infect HFF monolayers to determine the earliest changes in cell cycle proteins. Despite this limitation, we were able to show that increased production of VZV proteins corresponded with upregulation of cyclins A, B1, and D3 (Fig. 3). Interestingly, peak cyclin and CDK protein production were observed 3 days p.i., which correlated with peak infectious virus production (Fig. 1A). Using phosphonoacetic acid to inhibit the viral polymerase and block late gene expression and all kinetics downstream, infected HFFs did not express cyclin B1, indicating that upregulation is a late event that occurs after viral DNA

synthesis, whereas cyclin D3 expression was increased even with phosphonoacetic acid treatment (data not shown).

Contrary to our initial speculation, increased CDK activity in VZV-infected cells is not a result of decreased expression of the CKIs p21 and p27. In fact, infected cultures showed a reproducible increase in p27 compared to mock-infected cultures (Fig. 5). It has been postulated that p27 can, in addition to being a CKI, act as an adaptor protein for bringing together CDKs and their partner cyclins, increasing the probability of binding and consequent activity (12, 43). The elevated CDK activity found in VZV-infected cells in the presence of p21 and p27 lends credence to this idea. Alternatively, the CKIs may not be located near the CDK-cyclin complexes in infected cells. In support of the latter hypothesis, confocal microscopy demonstrated that p27 is cytoplasmic in infected cells, whereas in mock-infected cells it is nuclear (data not shown). This may explain its failure to inhibit CDKs, since nuclear CKIs are inhibitory (12, 14, 33).

Cyclins B1 and D3 increased more than other cell cycle proteins following VZV infection, and so their localization was examined by confocal immunofluorescence microscopy. Cyclin D3 was present in infected cell nuclei and apparently came after IE62 translation, as we observed cells with IE62 alone but saw cyclin D3 only in cells with IE62. The situation is slightly different for cyclin B1, in that its expression was not uniform across VZV-infected cultures. Some cells expressed cyclin B1 in the cytoplasm, and rare cells expressed condensed chromatin and nuclear cyclin B1. We speculate that uninfected cells expressing cyclin B1 around VZV plaques were present in the initial inoculum and settled into the monolayer and either completed one round of replication or became arrested in G_2/M phase. The flow cytometry results support this, since both mock- and VZV-infected cultures exhibit a small population of cells with 4N DNA content. However, within VZV plaques cyclin B1 was found in both the nucleus and cytoplasm of some, but not all, infected cells. There were also areas where IE62 protein was present and cyclin B1 was not. Therefore, cyclin B1 protein expression was not required before IE62 transcription and translation or for translocation of IE62 out of the nucleus. Colocalization of cyclin B1 and IE62 was most prominent in the middle of the plaque, where the cells were infected first and were assembling viral progeny for the longest period. Supporting this concept, cyclin B1 and B2 are normally most active in G_2/M phase when they are responsible for disassembling the nuclear envelope and the Golgi apparatus, respectively (18), although cyclin B2 was not overexpressed in VZV-infected cells. In cycling HFFs, cyclin B2 protein levels increased during G_2/M, when the Golgi apparatus must be divided between two daughter cells. This is further evidence that the virus does not induce general cyclin synthesis.

One function of CDK1/cyclin B1 is to break down the nuclear envelope in preparation for mitosis, yet this does not appear to occur in VZV-infected cells, suggesting that the cyclin B1 complex is redirected for different purposes, similar to the alterations in CDK4/cyclin D3. Capsids of VZV and other herpesviruses must penetrate the network of lamins to access the inner nuclear membrane, and this aspect of nuclear egress has become an important area of research. It has recently been shown that HSV infection of Hep-2 cells (an epithelial cell line) results in phosphorylation of lamin B, a nuclear membrane component (42). The authors demonstrated a connection between protein kinase C and lamin B phosphorylation that was partially reduced by a chemical inhibitor. This indicates that other kinases may work in concert with protein kinase C activity, including CDKs (15, 39). However, since cyclin B1 was predominantly cytoplasmic in VZV-infected HFFs, we are currently investigating whether cyclin B1 is present in the Golgi, where glycoproteins and IE62 are packaged into the virion tegument. Additional evidence that CDK1/cyclin B may have a role in virus assembly is that gI, located on Golgi and plasma membranes in infected cells, is phosphorylated by CDK1 in vitro and that this reaction is inhibited by roscovitine (57).

Other herpesviruses have previously been shown to subvert the cell cycle by inducing the production of cell cycle proteins out of order. HCMV causes the translocation of CDK2 from the cytoplasm to the nucleus in human fibroblasts and directly induces cyclin E transcription, resulting in an increase in cyclin E protein (8, 9). In addition, CDK2 was active in cells infected with HCMV, and this activity was inhibited by roscovitine, which also inhibited viral DNA synthesis (10). This demonstrates an important role for CDKs in HCMV replication. Like VZV, HCMV also increases cyclin B1 and cyclin A protein levels and induces CDK2 and CDK1 kinase activity while CDK2 and CDK1 protein levels remain steady (27). The result of these studies is a growing consensus that HCMV infection of human fibroblasts results in a G_1/S-phase arrest, allowing for viral replication while blocking competing cellular replication (11, 16, 53).

HSV-1 has been extensively studied in regard to its effects on host cell cycle proteins, although the use of cells other than fibroblasts makes comparisons to this work more difficult. The pocket protein p130 has been shown to be required for wild-type kinetics of viral replication using knockout murine cells, with deletion of the gene resulting in significantly decreased viral titers and delayed immediate-early and early gene products (20). Cyclins A and B and CDK1 protein were all downregulated in HSV-1 infected HeLa cells, but CDK1-associated kinase activity increased (2). It has been hypothesized that activation of CDK1 results from an interaction with the viral U_L42 protein and that this activity is used to recruit topoisomerase IIα for late gene expression (3, 4).

The specific functions of CDKs in VZV's life cycle, and in those of other herpesviruses, is unknown. The purpose of CDK activity may be to regulate cell functions that are important for viral replication by targeting host cell proteins or to phosphorylate viral proteins directly. One possible role for CDKs is stimulation of viral gene transcription through the function of CDK7 and CDK9 in the RNA polymerase II complex (19). It has also been shown that CDK1 can bind U_L42 in HSV-1 infected cells and phosphorylate it, implicating cellular kinases in the regulation of viral proteins (3). However, Davido et al. showed that roscovitine can inhibit ICP0 transactivating abilities without affecting its phosphorylation, suggesting that CDK phosphorylation of viral substrates is not the only way that HSV-1 requires CDK activity (13). These possible CDK functions are supported by the findings that CDK inhibitors prevent replication of VZV and all other herpesviruses tested (10, 50, 51). This suggests an important role for CDKs, probably at multiple stages of the viral life cycle.

This virally infected cell state sets a conundrum: how to separate DNA synthesis from the protein profile of the cell. Although CDKs are active in VZV-infected HFFs, putative substrates such as pRb family members are not phosphorylated, CKIs are abundant, and there does not seem to be cellular DNA synthesis. There are several possible explanations for this paradox: (i) This could be a result of a biochemically altered state, in that CDK activity in infected cells is different from CDK activity in cycling cells and substrate recognition is altered; (ii) VZV might biochemically alter cellular substrates to prevent binding to CDKs; (iii) phosphorylated substrates could be quickly degraded; or, most probably, (iv) CDK activity is being targeted to different cellular or viral components or subcellular locations. We are currently testing these possibilities, and early experiments indicate that at least one VZV protein is phosphorylated by CDKs (authors' observations). It will also be important to determine whether VZV activates transcription of cyclin genes, and, more specifically, how it may block origin firing and cellular DNA synthesis in the presence of positive regulators. In conclusion, we have shown how infection of a nondividing fibroblast monolayer by VZV affects cell cycle proteins, as well as demonstrating an apparent divergence of cellular DNA synthesis and the protein composition of a cell.

ACKNOWLEDGMENTS

We thank Paul R. Kinchington, University of Pittsburgh, for the IE62 antibodies and Ann Arvin, Stanford University, for the human antisera to VZV. Prabal Banerjee aided us with expertise in flow cytometry.

This work was supported by PHS AI052168 (J.F.M.).

REFERENCES

1. **Adams, P. D., X. Li, W. R. Sellers, K. B. Baker, X. Leng, J. W. Harper, Y. Taya, and W. G. Kaelin, Jr.** 1999. Retinoblastoma protein contains a C-terminal motif that targets it for phosphorylation by cyclin-cdk complexes. Mol. Cell. Biol. **19:**1068–1080.
2. **Advani, S. J., R. Brandimarti, R. R. Weichselbaum, and B. Roizman.** 2000. The disappearance of cyclins A and B and the increase in activity of the G_2/M-phase cellular kinase cdc2 in herpes simplex virus 1-infected cells require expression of the $\alpha22/U_S1.5$ and U_L13 viral genes. J. Virol. **74:**8–15.
3. **Advani, S. J., R. R. Weichselbaum, and B. Roizman.** 2001. cdc2 cyclin-dependent kinase binds and phosphorylates herpes simplex virus 1 U_L42 DNA synthesis processivity factor. J. Virol. **75:**10326–10333.
4. **Advani, S. J., R. R. Weichselbaum, and B. Roizman.** 2003. Herpes simplex virus 1 activates cdc2 to recruit topoisomerase II alpha for post-DNA synthesis expression of late genes. Proc. Natl. Acad. Sci. USA **100:**4825–4830.
5. **Arvin, A.** 1996. Varicella-zoster virus, p. 2547–2585. *In* B. N. Fields, D. M. Knipe, and P. M. Howley (ed.), Virology, 2nd ed. Lippincott-Raven, Philadelphia, Pa.
6. **Biswas, N., V. Sanchez, and D. H. Spector.** 2003. Human cytomegalovirus infection leads to accumulation of geminin and inhibition of the licensing of cellular DNA replication. J. Virol. **77:**2369–2376.
7. **Bradford, M. M.** 1976. A rapid and sensitive method for the quantitation of microgram quantities of protein utilizing the principle of protein-dye binding. Anal. Biochem. **72:**248–254.
8. **Bresnahan, W. A., E. A. Thompson, and T. Albrecht.** 1997. Human cytomegalovirus infection results in altered Cdk2 subcellular localization. J. Gen. Virol. **78:**1993–1997.
9. **Bresnahan, W. A., T. Albrecht, and E. A. Thompson.** 1998. The cyclin E promoter is activated by human cytomegalovirus 86-kDa immediate early protein. J. Biol. Chem. **273:**22075–22082.
10. **Bresnahan, W. A., I. Boldogh, P. Chi, E. A. Thompson, and T. Albrecht.** 1997. Inhibition of cellular Cdk2 activity blocks human cytomegalovirus replication. Virology **231:**239–247.
11. **Bresnahan, W. A., I. Boldogh, E. A. Thompson, and T. Albrecht.** 1996. Human cytomegalovirus inhibits cellular DNA synthesis and arrests productively infected cells in late G1. Virology **224:**150–160.
12. **Coqueret, O.** 2003. New roles for p21 and p27 cell-cycle inhibitors: a function for each cell compartment? Trends Cell Biol. **13:**65–70.
13. **Davido, D. J., D. A. Leib, and P. A. Schaffer.** 2002. The cyclin-dependent kinase inhibitor Roscovitine inhibits the transactivating activity and alters the posttranslational modification of herpes simplex virus type 1 ICP0. J. Virol. **76:**1077–1088.
14. **Denicourt, C., and S. F. Dowdy.** 2004. Cip/Kip proteins: more than just CDKs inhibitors. Genes Dev. **18:**851–855.
15. **Dessev, G., C. Iovcheva-Dessev, J. Bischoff, D. Beach, and R. Goldman.** 1991. A complex containing p34cdc2 and cyclin B phosphorylates the nuclear lamin and disassembles nuclei of clam oocytes in vitro. J. Cell Biol. **112:**523–533.
16. **Dittmer, D., and E. Mocarski.** 1997. Human cytomegalovirus infection inhibits G_1/S transition. J. Virol. **71:**1629–1634.
17. **Dowdy, S. F., P. W. Hinds, K. Louie, S. I. Reed, A. Arnold, and R. A. Weinberg.** 1993. Physical interaction of the retinoblastoma protein with human D cyclins. Cell **73:**499–511.
18. **Draviam, V. M., S. Orrechia, M. Lowe, R. Pardi, and J. Pines.** 2001. The localization of human cyclins B1 and B2 determines CDK1 substrate specificity and neither enzyme requires MEK to disassemble the Golgi apparatus. J. Cell Biol. **152:**945–958.
19. **Durand, L. O., S. J. Advani, A. P. W. Poon, and B. Roizman.** 2005. The carboxyl-terminal domain of RNA polymerase II is phosphorylated by a complex containing cdk9 and infected-cell protein 22 of herpes simplex virus 1. J. Virol. **79:**6757–6762.
20. **Ehmann, G. L., H. A. Burnett, and S. L. Bachenheimer.** 2001. Pocket protein p130/Rb2 is required for efficient herpes simplex virus type 1 gene expression and viral replication. J. Virol. **75:**7149–7160.
21. **Ekholm, S. V., and S. I. Reed.** 2000. Regulation of G_1 cyclin-dependent kinases in the mammalian cell cycle. Curr. Opin. Cell Biol. **12:**676–684.
22. **Ewen, M. E., H. K. Sluss, C. J. Sherr, H. Matsushime, J.-Y. Kato, and D. M. Livingston.** 1993. Functional interactions of the retinoblastoma protein with mammalian D-type cyclins. Cell **73:**487–497.
23. **Grose, C., W. Jackson, and J. Traugh.** 1989. Phosphorylation of varicella-zoster virus glycoprotein gpI by mammalian casein kinase II and casein kinase I. J. Virol. **63:**3912–3918.
24. **Gu, Y., J. Rosenblatt, and D. O. Morgan.** 1992. Cell cycle regulation of CDK2 activity by phosphorylation of Thr160 and Tyr15. EMBO J. **11:**3995–4005.
25. **Harbour, J. W., R. X. Luo, A. D. Santi, A. A. Postigo, and D. C. Dean.** 1999. Cdk phosphorylation triggers sequential intramolecular interactions that progressively block Rb functions as cells move through G1. Cell **98:**859–869.
26. **Hossain, A., T. Holt, J. Ciacci-Zanella, and C. Jones.** 1997. Analysis of cyclin-dependent kinase activity after herpes simplex virus type 2 infection. J. Gen. Virol. **78:**3341–3348.
27. **Jault, F., J. Jault, F. Ruchti, E. Fortunato, C. Clark, J. Corbeil, D. Richman, and D. Spector.** 1995. Cytomegalovirus infection induces high levels of cyclins, phosphorylated Rb, and p53, leading to cell cycle arrest. J. Virol. **69:**6697–6704.
28. **Kato, J., H. Matsushime, S. W. Hiebert, M. E. Ewen, and C. J. Sherr.** 1993. Direct binding of cyclin D to the retinoblastoma gene product (pRb) and pRb phosphorylation by the cyclin D-dependent kinase CDK4. Genes Dev. **7:**331–342.
29. **Kawaguchi, Y., K. Kato, M. Tanaka, M. Kanamori, Y. Nishiyama, and Y. Yamanashi.** 2003. Conserved protein kinases encoded by herpesviruses and cellular protein kinase cdc2 target the same phosphorylation site in eukaryotic elongation factor 1δ. J. Virol. **77:**2359–2368.
30. **Kenyon, T. K., J. I. Cohen, and C. Grose.** 2002. Phosphorylation by the varicella-zoster virus ORF47 protein serine kinase determines whether endocytosed viral gE traffics to the *trans*-Golgi network or recycles to the cell membrane. J. Virol. **76:**10980–10993.
31. **Koepp, D. M., J. W. Harper, and S. J. Elledge.** 1999. How the cyclin became a cyclin: regulated proteolysis in the cell cycle. Cell **97:**431–434.
32. **Li, C.-J., A. Vassilev, and M. L. DePamphilis.** 2004. Role for Cdk1 (Cdc2)/cyclin A in preventing the mammalian origin recognition complex's largest subunit (Orc1) from binding to chromatin during mitosis. Mol. Cell. Biol. **24:**5875–5886.
33. **Li, R., G. J. Hannon, D. Beach, and B. Stillman.** 1996. Subcellular distribution of p21 and PCNA in normal and repair-deficient cells following DNA damage. Curr. Biol. **6:**189–199.
34. **Lowe, M., C. Rabouilee, N. Nakamura, R. Watson, M. Jackman, E. Jamsa, D. Rahman, D. J. C. Pappin, and G. Warren.** 1998. Cdc2 kinase directly phosphorylates the *cis*-Golgi matrix protein GM130 and is required for Golgi fragmentation in mitosis. Cell **94:**783–793.
35. **Moffat, J. F., M. A. McMichael, S. A. Leisenfelder, and S. L. Taylor.** 2004. Viral and cellular kinases are potential antiviral targets and have a central role in varicella zoster virus pathogenesis. Biochim. Biophys. Acta **1697:**225–231.
36. **Moffat, J. F., L. Zerboni, P. R. Kinchington, C. Grose, H. Kaneshima, and A. M. Arvin.** 1998. Attenuation of the vaccine Oka strain of varicella-zoster virus and role of glycoprotein C in alphaherpesvirus virulence demonstrated in the SCID-hu mouse. J. Virol. **72:**965–974.
37. **Morgan, D. O.** 1997. Cyclin-dependent kinases: engines, clocks, and microprocessors. Annu. Rev. Cell Dev. Biol. **13:**261–291.
38. **Nakayama, K.-I., and K. Nakayama.** 1998. Cip/Kip cyclin-dependent kinase

inhibitors: brakes of the cell cycle engine during development. Bioessays **20:**1020–1029.
39. **Nigg, E. A.** 1992. Assembly-disassembly of the nuclear lamina. Curr. Opin. Cell Biol. **4:**105–109.
40. **Niizuma, T., L. Zerboni, M. H. Sommer, H. Ito, S. Hinchliffe, and A. M. Arvin.** 2003. Construction of varicella-zoster virus recombinants from parent Oka cosmids and demonstration that ORF65 protein is dispensable for infection of human skin and T cells in the SCID-hu mouse model. J. Virol. **77:**6062–6065.
41. **Ohi, R., and K. L. Gould.** 1999. Regulating the onset of mitosis. Curr. Opin. Cell Biol. **11:**267–273.
42. **Park, R., and J. D. Baines.** 2006. Herpes simplex virus type 1 infection induces activation and recruitment of protein kinase C to the nuclear membrane and increased phosphorylation of lamin B. J. Virol. **80:**494–504.
43. **Parry, D., D. Mahony, K. Wills, and E. Lees.** 1999. Cyclin D-CDK subunit arrangement is dependent on the availability of competing INK4 and p21 class inhibitors. Mol. Cell. Biol. **19:**1775–1783.
44. **Porter, L. A., and D. J. Donoghue.** 2003. Cyclin B1 and CDK1: nuclear localization and upstream regulators, p. 335–347. *In* L. Meijer, A. Jezequel, and M. Roberge (ed.), Progress in cell cycle research, vol. 5. Kluwer Academic Publishers, Roscoff, France.
45. **Preisinger, C., and F. A. Barr.** 2001. Signaling pathways regulating Golgi structure and function. Sci. STKE **2001:**pe38. [Online.] doi:10.1126/stke.2001.106.pe38.
46. **Salvant, B. S., E. A. Fortunato, and D. H. Spector.** 1998. Cell cycle dysregulation by human cytomegalovirus: influence of the cell cycle phase at the time of infection and effects on cyclin transcription. J. Virol. **72:**3729–3741.
47. **Sanchez, V., A. K. McElroy, and D. H. Spector.** 2003. Mechanisms governing maintenance of Cdk1/cyclin B1 kinase activity in cells infected with human cytomegalovirus. J. Virol. **77:**13214–13224.
48. **Schang, L. M., A. Bantly, M. Knockaert, F. Shaheen, L. Meijer, M. H. Malim, N. S. Gray, and P. A. Schaffer.** 2002. Pharmacological cyclin-dependent kinase inhibitors inhibit replication of wild-type and drug-resistant strains of herpes simplex virus and human immunodeficiency virus type 1 by targeting cellular, not viral, proteins. J. Virol. **76:**7874–7882.
49. **Schang, L. M., J. Phillips, and P. A. Schaffer.** 1998. Requirement for cellular cyclin-dependent kinases in herpes simplex virus replication and transcription. J. Virol. **72:**5626–5637.
50. **Schang, L. M., A. Rosenberg, and P. A. Schaffer.** 2000. Roscovitine, a specific inhibitor of cellular cyclin-dependent kinases, inhibits herpes simplex virus DNA synthesis in the presence of viral early proteins. J. Virol. **74:**2107–2120.
51. **Taylor, S. L., P. R. Kinchington, A. Brooks, and J. F. Moffat.** 2004. Roscovitine, a cyclin-dependent kinase inhibitor, prevents replication of varicella-zoster virus. J. Virol. **78:**2853–2862.
52. **Vernell, R., K. Helin, and H. Muller.** 2003. Identification of target genes of the p16INK4A-pRB-E2F pathway. J. Biol. Chem. **278:**46124–46137.
53. **Wiebusch, L., and C. Hagemeier.** 2001. The human cytomegalovirus immediate early 2 protein dissociates cellular DNA synthesis from cyclin-dependent kinase activation. EMBO J. **20:**1086–1098.
54. **Wiebusch, L., R. Uecker, and C. Hagemeier.** 2003. Human cytomegalovirus prevents replication licensing by inhibiting MCM loading onto chromatin. EMBO Rep. **4:**42–46.
55. **Woo, R. A., and R. Y. C. Poon.** 2003. Cyclin-dependent kinases and S phase control in mammalian cells. Cell Cycle **2:**316–324.
56. **Yam, C. H., T. K. Fung, and R. Y. C. Poon.** 2002. Cyclin A in cell cycle control and cancer. Cell. Mol. Life Sci. **59:**1317–1326.
57. **Ye, M., K. M. Duus, J. Peng, D. H. Price, and C. Grose.** 1999. Varicella-zoster virus Fc receptor component gI is phosphorylated on its endodomain by a cyclin-dependent kinase. J. Virol. **73:**1320–1330.